481

Dynamic combination resonance characteristics of doubly curved panels subjected to non-uniform tensile edge loading with damping

Ratnakar. S. Udar[†] and P. K. Datta[‡]

Department of Aerospace Engineering, Indian Institute of Technology, Kharagpur-721302, India

Abstract. The dynamic instability of doubly curved panels, subjected to non-uniform tensile in-plane harmonic edge loading $P(t) = P_s + P_d \cos\Omega t$ is investigated. The present work deals with the problem of the occurrence of combination resonances in contrast to simple resonances in parametrically excited doubly curved panels. Analytical expressions for the instability regions are obtained at $\Omega = \omega_m + \omega_n$, ($\Omega$ is the excitation frequency and ω_m and ω_n are the natural frequencies of the system) by using the method of multiple scales. It is shown that, besides the principal instability region at $\Omega = 2\omega_1$, where ω_1 is the fundamental frequency, other cases of $\Omega = \omega_m + \omega_n$, related to other modes, can be of major importance and yield a significantly enlarged instability region. The effects of edge loading, curvature, damping and the static load factor on dynamic instability behavior of simply supported doubly curved panels are studied. The results show that under localized edge loading, combination resonance zones are as important as simple resonance zones. The effects of damping show that there is a finite critical value of the dynamic load factor for each instability region below which the curved panels cannot become dynamically unstable. This example of simultaneous excitation of two modes, each oscillating steadily at its own natural frequency, may be of considerable interest in vibration testing of actual structures.

Keywords: parametric instability; combination resonance; the method of multiple scales; finite element method; tensile non-uniform edge loading; damping.

1. Introduction

Aircraft and spacecraft structures consist of large number of panel type elements, which are subjected to a variety of static & dynamic loads during the flight. Many other structures such as ships, bridges, vehicles and offshore structures also use panel type elements. These components are susceptible to a variety of time-dependent and time-independent in-plane as well as out-of-plane loads. Aircraft skin panels are usually subjected to non-uniform in-plane stresses caused by non-uniform loading at the edges. In many cases the loading is tensile in nature. It is interesting to note that the curved panels subjected to non-uniform tensile in-plane loading may also undergo tension buckling due to pockets of compressive zones developed within the curved panels. Induced buckling may be important in certain applications such as stressed panels in aircraft wing skin. These

---

† E-mail: sanjaysu1114@yahoo.co.in
‡ Professor, E-mail: pkdatta@aero.iitkgp.ernet.in

elements being thin are prone to buckling & dynamic instabilities under external loading. The structural instability may lead to large deflection or large amplitude vibrations of structural elements leading to local or global failures. Hence the study of static and dynamic behavior of the doubly curved panels subjected to tensile edge loading is of considerable importance.

The curved panels subjected to in-plane dynamic (periodic) forces experience resonant transverse vibrations under certain combinations of the natural frequency of transverse vibration, the frequency of the in-plane forcing function and the magnitude of the in-plane load. This phenomenon is called dynamic instability or parametric instability or parametric resonance. The spectrum of the values of parameters causing unstable motion is called the region of dynamic instability or parametric resonance. If the frequency of in-plane forcing function at parametric resonance has relation with only one natural frequency of transverse vibration of the curved panel, the resulting resonance is called simple resonance; otherwise it is called combination resonance.

In the analysis of the dynamic stability of a structure subjected to a periodic loading $P(t) = P_s + P_d \cos \Omega t$, it is shown that for certain relationship between the excitation frequency and the natural ones, the dynamic instability occurs in the sense that the amplitude of the response increases without bound. Parametric resonance in shell structures under periodic loads had been of considerable interest since the subject was studied by Bolotin (1964). Parametric instability of elastic structures (columns, plates and shells) with or without damping has been investigated by Bolotin (1964), where the instability regions were constructed by using the Fourier analysis. A perturbation technique was employed by Argento and Scott (1993) to study the dynamic instability of anisotropic circular cylindrical shells subjected to axial loading.

Tension buckling of rectangular sheets due to concentrated forces has been studied by Leissa and Ayoub (1989). The influence of damping on the dynamic behavior of the curved panels becomes more pronounced with the use of special damping treatment to enhance the damping properties of the structure for vibration control. Parametric excitation behavior of plates with damping subjected to uniform in-plane loading has been studied by Hutt and Salam (1971). Moorthy *et al.* (1990) studied the effect of damping on parametric instability of laminated composite plates with transverse shear deformation. The effect of damping on the dynamic instability behavior of beams has also been studied by Engel (1991). The effects of damping on the parametric instability behavior of plates under localized edge loading (compression or tension) are studied by Deolasi and Datta (1995). Recently, Sahu and Datta (2001) investigated the principle instability regions for the doubly curved panels subjected to non-uniform harmonic compressive loading using finite element method. In all these studies the principal instability region, at which $\Omega = 2\omega_1$ (ω_1 is the lowest natural frequency of the system) was derived and the effects of the aspect ratio, static in-plane force, boundary condition and thickness were investigated.

The existence of the combination resonance phenomenon is well established in dynamic instability studies. Bolotin's method (1964) is very common for obtaining the primary instability regions, but it cannot be used for solving combination resonance problems. Different authors Hsu (1963), Stupnicka (1978), Nayfeh and Mook (1979), Takahashi (1981) have proposed different methods for solving combination resonance problems. Iwatsubo *et al.* (1974) studied the simple and combination resonances of columns under periodic axial loads. Takahashi and Konishi (1988) analyzed the simple as well as combination resonances of rectangular plates subjected to an in-plane sinusoidal linearly varying force by using harmonic balance method. Ostiguy *et al.* (1993) investigated the occurrence of simultaneous and combination resonances in multi-degree-of-freedom systems subjected to parametric excitation by using the generalized asymptotic method. Saha *et al.* (1997)

have studied the simple and combination resonances of a rectangular plate on non-homogeneous Winkler foundation, subjected to uniform compressive in-plane (biaxial) dynamic loads. Deolasi and Datta (1997) have studied the simple and combination resonances of isotropic rectangular plates subjected to non-uniform edge loading with damping. Kar and Sujata (1991) investigated the simple and combination resonances of tapered symmetric sandwich beam subjected to periodic axial force by using the method of multiple scales (MMS). Cederbaum (1991) investigated the simple and combination resonances of shear deformable laminated plates, modeled within HSDT subjected to biaxial periodic loading by using the method of multiple scales (MMS). Mond and Cederbaum (1992) investigated the simple and combination resonance zones of anti-symmetric laminated plates using the method of multiple scales (MMS). Cederbaum (1992) analyzed the simple and combination resonance characteristics of shear deformable circular cylindrical shell subjected to uniform periodic axial loading. Argento (1993) investigated the simple and combination resonance characteristics of composite circular cylindrical shell subjected to combined axial and torsional loading. Lee and Kim (1995) studied the combination resonances of a clamped circular plate with three mode interaction by using the method of multiple scales (MMS). Kim and Choo (1998) investigated the simple and combination resonance (sum and difference) characteristics of free-free Timoshenko beam subjected to a pulsating follower force using the method of multiple scales (MMS). Choo and Kim (2000) also studied the simple and combination resonance (sum and difference) characteristics of isotropic and non-symmetric laminated plates with four free edges subjected to pulsating follower forces by using the method of multiple scales (MMS). Recently, investigations of the effect of damping on the simple and combination resonance (sum and difference) characteristics of planar elastic panel subjected to the supersonic gas flow along with perturbed gas pressure and the initial compression in the middle plane of the panel have been made by Bolotin *et al.* (2002). However there is no reference available in the literature on the simple and combination resonance characteristics of the doubly curved panels subjected to non-uniform tensile in-plane harmonic edge loading with damping.

The present paper deals with the study of the simple and combination resonances of the doubly curved panels (Fig. 1) subjected to partial and concentrated edge loading cases as shown in Fig. 2. The first order shear deformation theory is used to model the curved panels, considering the effects of transverse shear deformation and rotary inertia. The theory used is extended from the dynamic, shear deformable theory based on the Sanders' first approximation for doubly curved shells, which can be reduced to Love's and Donnell's theories by means of tracers. Finite element technique is applied for obtaining the non-uniform initial stress distribution and also to obtain the equilibrium equation for the flexural motion of the curved panel. Modal transformation is applied to transform the equilibrium equation into a suitable form. The method of multiple scales (Nayfeh 1973, Nayfeh and Mook 1979) is applied to obtain the boundaries of simple and combination resonance zones.

2. Analysis

An eight-noded curved isoparametric quadratic element with five degrees of freedom u, v, w, θ_x and θ_y at each node is employed in the present analysis. The application of the finite element method to the curved panel subjected to in-plane loading in the presence of damping yields the following equation of motion in a matrix form

$$[M]\{\ddot{q}\} + [C]\{\dot{q}\} + [K]\{q\} - P[S]\{q\} = 0 \qquad (1)$$

The stress stiffness matrix $[S]$ is essentially a result of the initial stress distribution within the curved panel, taking out P as common factor. Partial edge loading causes non-uniform initial stress distribution within the curved panel. Non-uniform stress distribution is taken care for computing $[S]$ by evaluating initial stresses at Gauss sampling points and using them in Gauss-quadrature numerical integration.

For static stability or buckling problem, Eq. (1) reduces to

$$[K]\{q\} - P_{cr}[S]\{q\} = 0 \qquad (2)$$

where P_{cr} is the static buckling load and $\{q\}$ gives the mode shapes of buckling.

For the free vibration problem without damping Eq. (1) can be expressed as

$$[[K] - P[S]]\{q\} - \omega^2[M]\{q\} = 0 \qquad (3)$$

where ω is the natural frequency of vibration and $\{q\}$ gives the normal modes of vibration.

Both Eqs. (2) and (3) are eigenvalue problems. The solutions to these equations give eigenvalues P_{cr} and ω^2 respectively and corresponding eigenvectors $\{q\}$. These eigenvalue problems can be effectively solved by the sub-space iteration method for the first few modes of practical interest of buckling and vibration.

2.1 Dynamic stability problem

In the dynamic stability problem the edge load $P(t)$ is periodic and is expressed in the form

$$P(t) = P_s + P_d \cos \Omega t \qquad (4)$$

$P(t)$ can also be expressed as

$$P(t) = \alpha P_{cr} + \beta P_{cr} \cos \Omega t \qquad (5)$$

where $\alpha = P_s/P_{cr}$ and $\beta = P_d/P_{cr}$ are termed as the static and dynamic load factors respectively.

Substituting Eq. (5) into Eq. (1) leads to

$$[M]\{\ddot{q}\} + [C]\{\dot{q}\} + [K]\{q\} - \alpha P_{cr}[S]\{q\} - \beta P_{cr} \cos \Omega t[S]\{q\} = 0 \qquad (6)$$

For given values of α, β and Ω, the solution to Eq. (6) is either bounded or unbounded. The spectrum of the values of these parameters for which the solution is unbounded gives the region of dynamic instability, corresponding to simple resonance case.

2.2 Perturbation analysis

The boundaries of the simple and combination parametric resonance zones are obtained by using the method of multiple scales (MMS) used in perturbation analysis, which was proposed by Nayfeh

(1973) and Nayfeh and Mook (1979). Before applying the method of multiple scales, Eq. (6) is modified into a suitable form by means of modal transformation. It is assumed that the first few normal modes of undamped free vibration of the curved panel are adequate to define the response of the curved panel to periodic edge loading.

Applying the modal transformation, Eq. (6) is modified to the following form

$$\{\ddot{\xi}\} + [\hat{C}]\{\dot{\xi}\} + [\Lambda]\{\xi\} + 2\varepsilon\cos\Omega t[\hat{S}]\{\xi\} = 0 \qquad (7)$$

where

$$[\hat{C}] = [\Phi]^T[C][\Phi], \quad [\Lambda] = [\Phi]^T[[K] - \alpha P_{cr}[S]][\Phi], \quad \varepsilon = \beta/2 \text{ and } [\hat{S}] = -P_{cr}[\Phi]^T[S][\Phi] \qquad (8)$$

$[\Phi]$ is the modal matrix containing first M normal modes of free vibration problem under the edge load αP_{cr} and $\{\xi\}$ is the vector of normal co-ordinates. $[\Lambda]$ is a diagonal matrix containing the squares of the first M natural frequencies ω_i, $i = 1, 2, ..., M$, in the diagonal elements.

The modal damping matrix $[\hat{C}]$ can be defined at this stage. It is reasonable to assume $[\hat{C}]$ to be diagonal matrix which gives a desired modal damping ratio in each mode of free vibration (Bolotin 1964).

The damping matrix $[\hat{C}]$ can be expressed as

$$[\hat{C}] = 2[\zeta][\overline{\Lambda}]^{1/2} \qquad (9)$$

where $[\zeta]$ is diagonal matrix containing modal damping ratios in the diagonal elements and $[\overline{\Lambda}]$ is also a diagonal matrix which contains squares of natural frequencies of vibration in absence of edge loading ($\alpha = \beta = 0$) in the diagonal elements. The diagonal element of $[\hat{C}]$, $\hat{C}_{ii}$ can be termed as the modal damping coefficient in the corresponding mode.

Eq. (7) can be written in the component form

$$\ddot{\xi}_m + 2\zeta\omega_m\dot{\xi}_m + \omega_m^2\xi_m + 2\varepsilon\cos\Omega t\sum_{n=1}^{M}\hat{S}_{mn}\xi_n = 0 \qquad m, n = 1, 2, ..., M \qquad (10)$$

The last term on the left hand side represents the coupling of the dynamical load to the normal modes of the system. The presence of these coupling terms prevents obtaining the exact analytical solutions for Eq. (10). However, since the amplitude of the dynamical load (ε) is assumed to be small, a perturbation scheme can be introduced in order to investigate its effect on the stability of the curved panels.

The multiscale analysis is based on the observation that the system described by Eq. (10) varies on different distinct time scales. As a result the time derivatives in Eq. (10) are replaced by following partial derivatives:

$$\frac{d\xi}{dT_0} = \frac{\partial\xi}{\partial T_0} + \varepsilon\frac{\partial\xi}{\partial T_1} + \varepsilon^2\frac{\partial\xi}{\partial T_2} + ... = D_0 + \varepsilon D_1 + \varepsilon^2 D_2 + ... \qquad (11)$$

ξ is expanded in power series in ε in the following way:

$$\xi_m = \xi_{m0}(T_0, T_1, T_2) + \varepsilon\xi_{m1}(T_0, T_1, T_2) + \varepsilon^2\xi_{m2}(T_0, T_1, T_2) + ... \qquad (12)$$

Substituting Eqs. (11) and (12) into Eq. (10) and equating like powers of ε, in the absence of damping second order terms result in the following equations

$$D_0^2 \xi_{m0} + \omega_m^2 \xi_{m0} = 0 \tag{13}$$

$$D_0^2 \xi_{m1} + \omega_m^2 \xi_{m1} = -2D_0 D_1 \xi_{m0} - \sum_s \hat{S}_{ms} \xi_{s0} [\exp(i\Omega T_0) + CC] \tag{14}$$

$$D_0^2 \xi_{m2} + \omega_m^2 \xi_{m2} = -2D_0 D_2 \xi_{m0} - D_1^2 \xi_{m0} - 2D_0 D_1 \xi_{m1} - \sum_s \hat{S}_{ms} \xi_{s1} [\exp(i\omega_m T_0)] + CC \tag{15}$$

2.2.1 The case Ω near $\omega_m + \omega_n$

The expressions for the boundary frequencies of various kinds of resonance zones can be derived by using the MMS. When the frequency of the excitation is close to the sum of two natural frequencies of the system, a combination resonance of summed type exists between the various modes. The nearness of Ω to $\omega_m + \omega_n$ can be expressed by introducing the detuning parameter σ, that is defined by

$$\Omega = \omega_m + \omega_n + \varepsilon\sigma \tag{16}$$

2.2.2 Second order expansion

The general solution of Eq. (13) can be written in the form

$$\xi_{m0} = A_m(T_1, T_2)\exp(i\omega_m T_0) + CC \tag{17}$$

where CC represents the complex conjugate of the preceding terms.

Substituting Eq. (17) into Eq. (14), the particular solution of the equation can be written as

$$\xi_{m1} = \sum_s \hat{S}_{ms} A_s \left\{ \frac{\exp[i(\omega_s + \Omega)T_0]}{(\omega_s + \Omega)^2 - \omega_m^2} + \frac{\exp[i(\omega_s - \Omega)T_0]}{(\omega_s - \Omega)^2 - \omega_m^2} \right\} + CC \tag{18}$$

Substituting Eqs. (17) and (18) into Eq. (15) and eliminating the non-secular terms from it, yields the following equations

$$2i\omega_m D_2 A_m + D_1^2 A_m + 2\omega_m \hat{\chi}_m A_m = 0 \tag{19}$$

$$2i\omega_n D_2 A_n + D_1^2 A_n + 2\omega_n \hat{\chi}_n A_n = 0 \tag{20}$$

where

$$\hat{\chi}_m = \frac{1.0}{2\omega_m} \left[\sum_s \frac{\hat{S}_{ms}\hat{S}_{sm}}{[(\omega_m + \Omega)^2 - \omega_s^2]} + \sum_{s \neq n} \frac{\hat{S}_{ms}\hat{S}_{sm}}{[(\omega_m - \Omega)^2 - \omega_s^2]} \right] \tag{21}$$

$$\hat{\chi}_n = \frac{1.0}{2\omega_n} \left[\sum_s \frac{\hat{S}_{ns}\hat{S}_{sn}}{[(\omega_n + \Omega)^2 - \omega_s^2]} + \sum_{s \neq m} \frac{\hat{S}_{ns}\hat{S}_{sn}}{[(\omega_n - \Omega)^2 - \omega_s^2]} \right] \tag{22}$$

Eqs. (19) and (20) can be written in the form

$$D_1^2 A_m = \frac{1}{4}\Lambda_{mn}A_m - \frac{\sigma \hat{S}_{mn}}{2\omega_m}\overline{A}_n \exp(i\sigma T_1) \tag{23}$$

$$D_1^2 A_n = \frac{1}{4}\Lambda_{mn}A_n - \frac{\sigma \hat{S}_{nm}}{2\omega_n}\overline{A}_m \exp(i\sigma T_1) \tag{24}$$

where

$$\Lambda_{mn} = \frac{\hat{S}_{mn}\hat{S}_{nm}}{\omega_m\omega_n} \tag{25}$$

Substituting Eqs. (23) and (24) into Eqs. (19) and (20) yields

$$2i\omega_m D_2 A_m + \left(\frac{1}{4}\Lambda_{mn} + 2\omega_m\hat{\chi}_m\right)A_m - \frac{\sigma \hat{S}_{mn}}{2\omega_m}\overline{A}_n\exp(i\sigma T_1) = 0 \tag{26}$$

$$2i\omega_n D_2 A_n + \left(\frac{1}{4}\Lambda_{mn} + 2\omega_n\hat{\chi}_n\right)A_n - \frac{\sigma \hat{S}_{nm}}{2\omega_n}\overline{A}_m\exp(i\sigma T_1) = 0 \tag{27}$$

It can be easily verified that Eqs. (26) and (27) are the first two terms in the multiple scales expansion of

$$2i\omega_m\frac{dA_m}{dt} + \varepsilon\left(1 - \frac{\varepsilon\sigma}{2\omega_m}\right)\hat{S}_{mn}\overline{A}_n\exp(i\varepsilon\sigma T_0) + \varepsilon^2\left(\frac{1}{4}\Lambda_{mn} + 2\omega_m\hat{\chi}_m\right)A_m = 0 \tag{28}$$

$$2i\omega_n\frac{dA_n}{dt} + \varepsilon\left(1 - \frac{\varepsilon\sigma}{2\omega_n}\right)\hat{S}_{nm}\overline{A}_m\exp(i\varepsilon\sigma T_0/2) + \varepsilon^2\left(\frac{1}{4}\Lambda_{mn} + 2\omega_n\hat{\chi}_n\right)A_n = 0 \tag{29}$$

Eqs. (28) and (29) admit a nontrivial solution, which are expressed in the form

$$A_m = a_m\exp[i\varepsilon(\lambda + \sigma)T_0] \quad \text{and} \quad A_n = a_n\exp(-i\varepsilon\overline{\lambda}T_0) \tag{30}$$

Substituting Eq. (30) into Eqs. (28) and (29) and by using the condition of solvability, it yields

$$\lambda^2 + (\sigma + \varepsilon\gamma_1)\lambda + \frac{1}{4}\Lambda_{mn} + \varepsilon\sigma\gamma_2 = 0 \tag{31}$$

$$\text{where } \gamma_1 = \frac{1}{8}\Lambda_{mn}\left(\frac{1}{\omega_n} - \frac{1}{\omega_m}\right) + \hat{\chi}_n - \hat{\chi}_m \text{ and } \gamma_2 = \hat{\chi}_n - \frac{\Lambda_{mn}}{8\omega_m} \tag{32}$$

Solving Eq. (31), it gives

$$\lambda = -\frac{1}{2}\left\{\sigma + \varepsilon\gamma_1 \pm [(\sigma + \varepsilon\gamma_1)^2 - \Lambda_{mn} - 4\varepsilon\sigma\gamma_2]^{1/2}\right\} \tag{33}$$

The transition curves correspond to the vanishing of radical in Eq. (33)

$$(\sigma + \varepsilon\gamma_1)^2 = (\Lambda_{mn} + 4\varepsilon\sigma\gamma_2) \tag{34}$$

By substituting Eq. (32) into Eq. (34), Eq. (34) can be written as

$$A\sigma^2 + B\sigma + C = 0 \tag{35}$$

where

$$A = \left[1 - \frac{\varepsilon^2 \Lambda_{mn}}{4\omega_m \omega_n}\right], \quad B = \varepsilon\left[\frac{\Lambda_{mn}}{4}\left(\frac{1}{\omega_m} + \frac{1}{\omega_n}\right) - 2(\hat{\chi}_m + \hat{\chi}_n)\right] \tag{36}$$

and

$$C = -\Lambda_{mn} + \varepsilon^2\left[(\hat{\chi}_m + \hat{\chi}_n) + \frac{\Lambda_{mn}}{8}\left(\frac{1}{\omega_m} + \frac{1}{\omega_n}\right)\right]^2 \tag{37}$$

In the presence of damping

$$A = \left[\frac{4\hat{C}_{mm}\hat{C}_{nn}}{(\hat{C}_{mm} + \hat{C}_{nn})^2} - \frac{\varepsilon^2 \Lambda_{mn}}{4\omega_m \omega_n}\right] \tag{38}$$

$$B = \varepsilon\left[\frac{8\hat{C}_{mm}\hat{C}_{nn}(\hat{\chi}_m + \hat{\chi}_n)}{(\hat{C}_{mm} + \hat{C}_{nn})^2} + \frac{\Lambda_{mn}}{2}\left(\frac{1}{\omega_m} + \frac{1}{\omega_n}\right)\right] \tag{39}$$

$$C = -\left[\Lambda_{mn} - \frac{\hat{C}_{mm}\hat{C}_{nn}}{\varepsilon^2} - 4\varepsilon^2\left\{\hat{\chi}_m\hat{\chi}_n - \frac{(\hat{C}_{mm}\hat{\chi}_n - \hat{C}_{nn}\hat{\chi}_m)^2}{(\hat{C}_{mm} + \hat{C}_{nn})^2}\right\} - 4\varepsilon\left\{\frac{(\hat{C}_{nn}\hat{\chi}_m - \hat{C}_{mm}\hat{\chi}_n)(\hat{\chi}_m - \hat{\chi}_n)}{(\hat{C}_{mm} + \hat{C}_{nn})}\right\}\right] \tag{40}$$

$$2\hat{\chi}_m\omega_m = -\frac{\Lambda_{mn}}{4} + \frac{\hat{C}_{mm}^2}{4\varepsilon^2} + \left[\sum_s \frac{\hat{S}_{ms}\hat{S}_{sm}}{[\omega_s^2 - (\Omega + \omega_m)^2]} + \sum_{s \neq n}\frac{\hat{S}_{ms}\hat{S}_{sm}}{[\omega_s^2 - (\Omega - \omega_m)^2]}\right] \tag{41}$$

$$2\hat{\chi}_n\omega_n = -\frac{\Lambda_{mn}}{4} + \frac{\hat{C}_{nn}^2}{4\varepsilon^2} + \left[\sum_s \frac{\hat{S}_{ns}\hat{S}_{sn}}{[\omega_s^2 - (\Omega + \omega_n)^2]} + \sum_{s \neq m}\frac{\hat{S}_{ns}\hat{S}_{sn}}{[\omega_s^2 - (\Omega - \omega_n)^2]}\right] \tag{42}$$

The two roots of Eq. (35) correspond to two boundaries of the dynamic instability region. The case $m = n$ gives the simple resonance zone and the case $m \neq n$ gives the combination resonance zone. The critical dynamic load factor, β^* corresponds to the value of β for which the expression $B^2 - 4AC$ is equal to zero. For the values of β below β^*, Eq. (35) gives complex roots which means that dynamic instability cannot occur.

The sum type and the difference type combination resonances cannot exist simultaneously for any pair of natural frequencies ω_m and ω_n. It can be stated that the difference type combination resonance exists, when $\hat{S}_{mn}$ and $\hat{S}_{nm}$ have different signs as elaborated by Iwatsubo *et al.* (1974), Nayfeh and Mook (1979) and Cederbaum (1991). Again the combination resonance of difference type does not appear in the case of the conservative loading due to the symmetry of $[\hat{S}]$ as explained by Takahashi (1981) and Kim and Choo (1998).
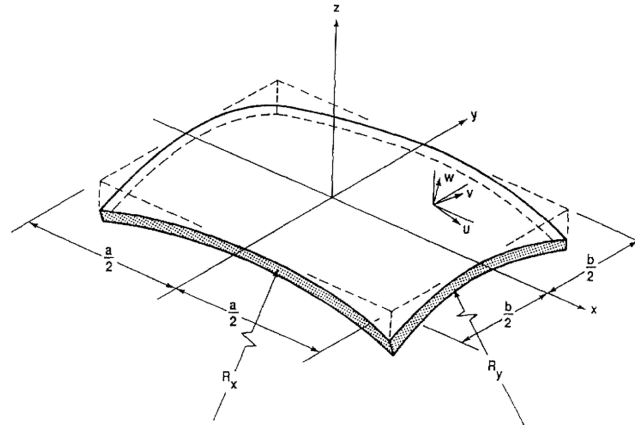
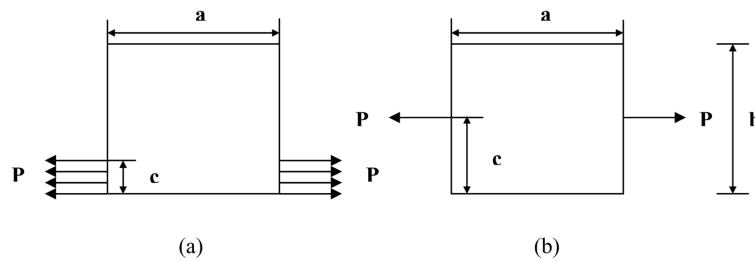Fig. 1 Geometry and co-ordinate system of a doubly curved panel

(a)   (b)

Fig. 2 (a) Tensile partial edge loading at one end (b) Tensile concentrated edge loading

3. Results and discussions

3.1 Problem definition

The basic configuration of the problem considered here is isotropic doubly curved panels (Fig. 1) subjected to tensile in–plane localized edge loading of different types as shown in Fig. 2. The boundaries of the panel are simply supported along all the edges unless otherwise stated. In the present analysis, panels of various geometries such as spherical $(R_y/R_x = 1)$, cylindrical $(R_y/R_x = 0)$ and hyperbolic paraboloidal $(R_y/R_x = -1)$ panels, with ratios of a/R_x and b/R_y as (0.2,0.2), (0.0,0.2) and (–0.2,0.2) respectively, aspect ratio $a/b = 1$ and breadth to thickness ratio $b/h = 100$ are considered unless otherwise stated for the analysis. In this analysis the tensile buckling load corresponding to the concentrated load acting at the corner of the curved panel $(c/b = 0)$ is taken as reference load. For different geometries, corresponding reference value is assigned.

3.2 Computer program

A computer program has been developed to perform all the necessary computations. Element elastic stiffness matrices are obtained with 2×2 Gauss sampling points to avoid possible shear locking. Element mass matrices are obtained with 2×2 Gauss sampling points, as higher order integration is often unnecessary. The geometric stiffness matrix is essentially a function of the in-

plane stress distribution in the element due to applied edge loading. Since the stress field is non-uniform, plane stress analysis is carried out using finite element technique to determine the stresses at 3×3 Gauss sampling points.

Element matrices are assembled into global matrices by using skyline technique. Subspace iteration method is adopted throughout to solve the eigenvalue problems. The first forty normal modes of free vibration are used for modal transformation of Eq. (6) into Eq. (7). Eq. (7) is considerably smaller and is in a form suitable for application of the MMS. The flow chart of the computer program is shown in Fig. 1 of the appendix-I. The instability regions are obtained from Eqs. (16) and (35) and the results are expressed in non-dimensional form. The non-dimensional load γ and non-dimensional frequency $\overline{\omega}$ are defined as shown in Table 1.

Convergence studies are carried out for the free vibration of clamped-free-free-free doubly curved panels and the results are compared with Leissa *et al.* (1983) as shown in Table 2. A mesh of 10×10 shows a good convergence of the numerical solutions for the free vibration of the doubly curved panels.

Table 1 Non-dimensional frequency and buckling parameters for isotropic shells

S. No	Non-dimensional parameters	Isotropic shells
1	Natural frequency $\overline{\omega}$	$\omega a^2 \sqrt{\rho h/D}$
2	Buckling load (γ)	$P_{cr} b^2/D$

Where $D = Eh^3/12(1 - v^2)$ and $G = E/2(1 + v)$

Table 2 Convergence of non-dimensional free vibration frequencies for C-F-F-F square doubly curved panels/shells

Mesh division	Non-dimensional frequencies of shells		
	Cylindrical	Spherical	Hyperbolic paraboloid
4×4	8.3836	6.6529	6.6071
6×6	8.3726	6.5955	6.5192
8×8	8.3678	6.5786	6.5014
10×10	8.3653	6.5747	6.4969
Leissa *et al.* (1983)	(8.3683)	(6.5854)	(6.5038)

Table 3 Comparison of non-dimensional fundamental frequencies for a simply supported doubly curved panels/shells

a/h	a/R_x	a/R_y	Non-dimensional $\omega h \sqrt{\rho/G}$	
			Present FEM	Matsunaga (1999)
10	0.0	0.0	0.09302	0.09315
	0.2	0.2	0.09821	0.09826
	0.0	0.2	0.09425	0.09436
	−0.2	0.2	0.09264	0.09276
20	0.0	0.0	0.02386	0.02387
	0.2	0.2	0.02873	0.02872
	0.0	0.2	0.02514	0.02515
	−0.2	0.2	0.02376	0.02378

Table 4 Comparison of non-dimensional tensile buckling loads for a simply supported
square plate under concentrated edge loading

| a/b | c/b | Non-dimensional tensile buckling loads | |
		Present FEM	Leissa & Ayoub (1989)
1.0	0.5	597.1244	614.0000
2.0	0.5	628.6746	638.0000

Table 5 Non-dimensional tensile buckling loads for a simply supported square doubly curved
panels/shells under partial edge loading at one end

| c/b | Non-dimensional tensile buckling loads of shells | | | |
	Flat	Spherical	Cylindrical	Hyp-Paraboloid
0.1	604	806	710	660
0.2	1017	1249	1127	1080
0.3	1663	1979	1794	1737
0.4	2957	3336	3099	3045
0.5	6039	6345	6156	6095
0.6	10499	10757	10501	10716
0.7	6792	7130	6794	7065
0.8	6310	6656	6311	6596
0.9	11918	12253	11918	12211

Table 6 Non-dimensional tensile buckling loads for a simply supported square doubly curved
panels/shells under concentrated edge loading

| c/b | Non-dimensional tensile buckling loads of shells | | | |
	Flat	Spherical	Cylindrical	Hyp-Paraboloid
0.1	1031	1266	1143	1095
0.2	1840	1985	1856	1936
0.3	828	997	839	942
0.4	628	803	637	741
0.5	597	776	607	708
0.6	628	803	637	741
0.7	828	997	839	942
0.8	1840	1985	1856	1936
0.9	1031	1266	1143	1095
1.0	380	532	466	428

For further validation of the program, the natural frequencies of the doubly curved panels with different a/h ratios are compared with the results of Matsunaga (1999) as shown in Table 3. Along with the free vibration studies, the results of buckling of the plates subjected to a pair of tensile concentrated loads as special case of non-uniform loading are compared with the results of Leissa and Ayoub (1989) as shown in Table 4. The present finite element based plate buckling results match well with the results given by Leissa and Ayoub (1989). Non-dimensional buckling loads of the doubly curved panels subjected to tensile partial and concentrated edge loadings with different load band widths are shown in Table 5 and Table 6 respectively.
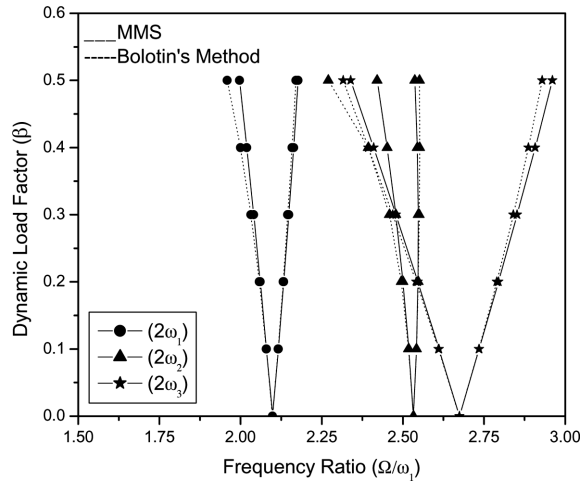
Fig. 3 Comparison of simple resonances of spherical
       panel subjected to partial edge loading at one
       end, obtained by Bolotin's Method and MMS
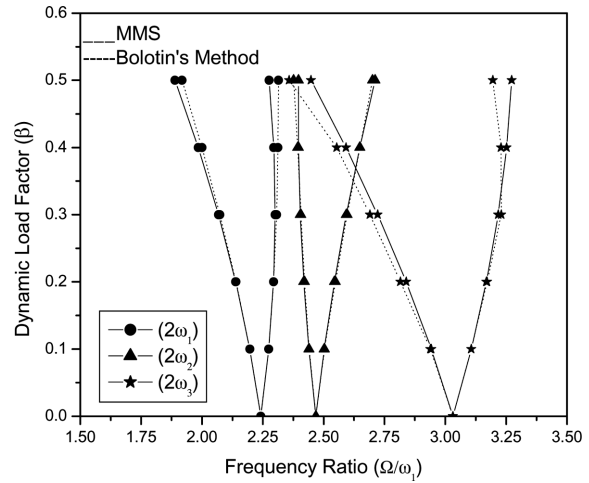   ($c/b = 0.2$, $\alpha = 0.2$)

Fig. 4 Same as Fig. 3, but for concentrated edge
       loading near the centre ($c/b = 0.4$)

Before applying the method of multiple scales (MMS) for obtaining the detailed results, the validity of the MMS is checked by comparing the simple resonance zones obtained by the MMS with those obtained by Bolotin's Method. The results obtained by both methods almost coincide for small values of β and differ slightly for higher values of β, which are shown in Figs. 3 and 4.

After checking the validity of the method of multiple scales (MMS) for simply supported spherical panels subjected to partial edge loading at one end and concentrated edge loading near the centre, the MMS program developed in this paper is used to study the effects of different parameters on the dynamic instability behavior of the curved panels.

3.3 Effect of edge loading

It can be observed from Figs. 5-10 that the widths of simple resonance zones are smaller in general for the partial edge loading of small bandwidth ($c/b = 0.2$) or for concentrated edge loading at one end ($c/b = 0.0$) for the doubly curved panels in comparison to large bandwidth ($c/b = 0.8$) of partial edge loading or for concentrated edge loading near the centre ($c/b = 0.4$). This may be due to the fact that the edge restraints provide a stabilizing effect on the simple resonance behavior as in the case of buckling characteristics. The widths of simple resonance zones are very large, when the curved panels are subjected to concentrated edge loading near the centre ($c/b = 0.4$), because the edge restraints are not very effective in this case. It is observed that under tensile loading the primary instability regions shift inward on the frequency ratio axis for small values of load bandwidth ($c/b = 0.2$) or for concentrated edge loading at one end ($c/b = 0.0$), indicating the onset of instability much earlier in comparison to large values of load bandwidth ($c/b = 0.8$) or for concentrated edge loading near the centre ($c/b = 0.4$) in contrast to the corresponding compressive loading cases (Figs. 11 and 12). This is due to the fact that for small values of load bandwidth ($c/b = 0.2$) or for concentrated edge loading at one end ($c/b = 0.0$), the compressive zones on the
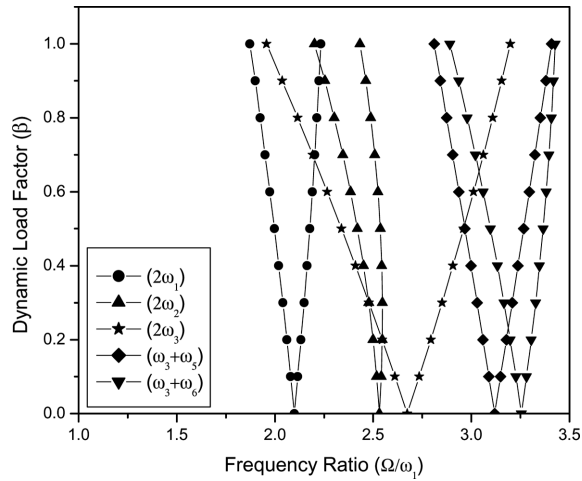
Fig. 5 Regions of simple and combination resonances of spherical panel subjected to tensile partial edge loading at one end ($c/b = 0.2$, $\alpha = 0.2$)
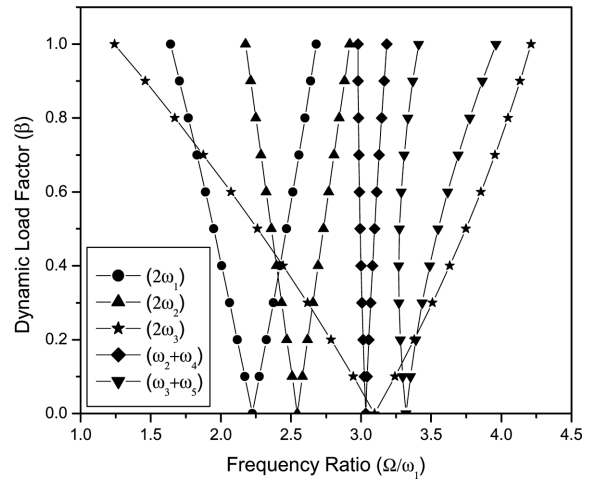

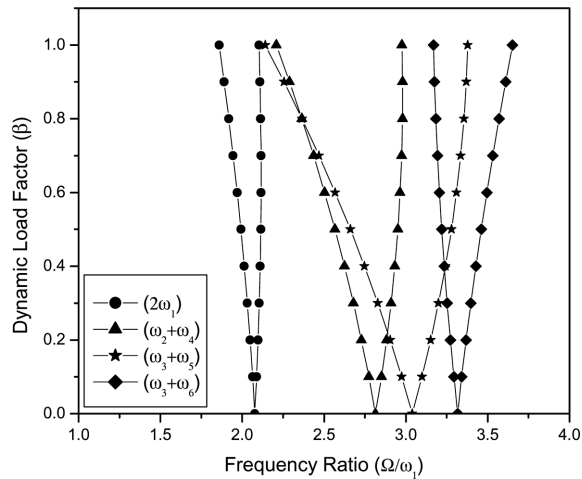Fig. 6 Same as Fig. 5, but for ($c/b = 0.8$)

Fig. 7 Regions of simple and combination resonances of spherical panel subjected to tensile concentrated edge loading at one end ($c/b = 0.0$, $\alpha = 0.2$)
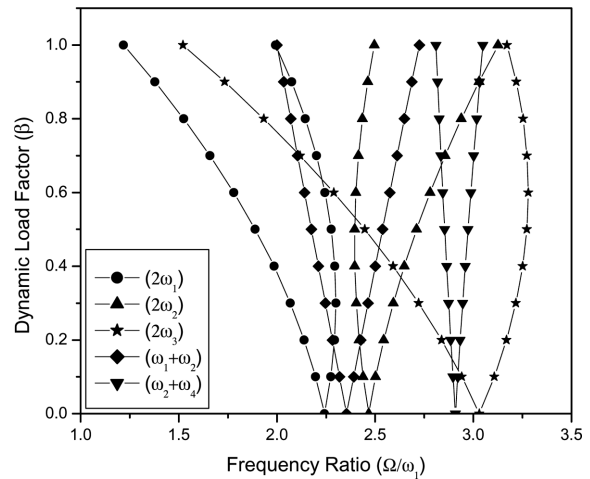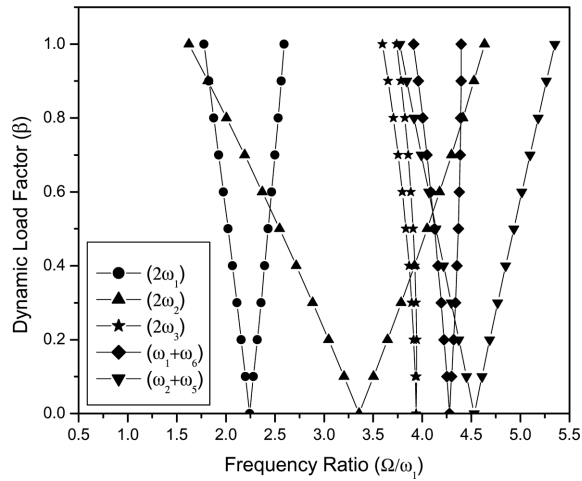

Fig. 8 Same as Fig. 7, but for ($c/b = 0.4$)

curved panels are much wider, causing the instability effects to appear earlier.

Further, it is observed from Figs. 5-10 that the widths of combination resonance zones are comparable to those of simple resonance zones for partial edge loading of small bandwidth and for concentrated edge loading of the doubly curved panels. It is shown that the widths of the combination resonance zones are large for the partial edge loading of small bandwidth ($c/b = 0.2$) or for concentrated edge loading ($c/b = 0.0, 0.4$) of the doubly curved panels and are very small for nearly uniform edge loading ($c/b = 0.8$) in contrast to the simple resonance zones. This may be due

Fig. 9 Regions of simple and combination resonances of cylindrical panel subjected to tensile partial edge loading at one end ($c/b = 0.2$, $\alpha = 0.2$)
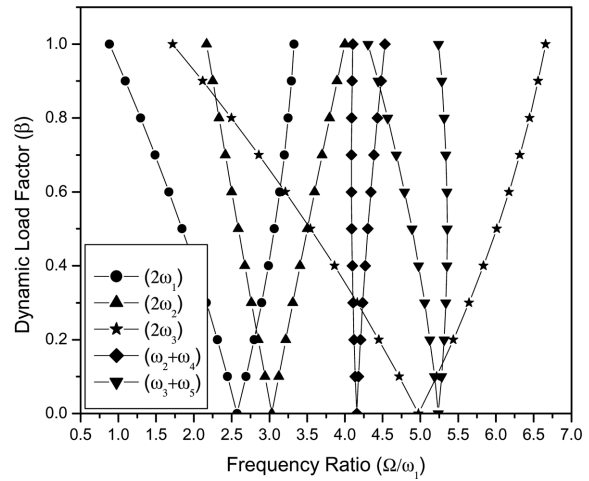

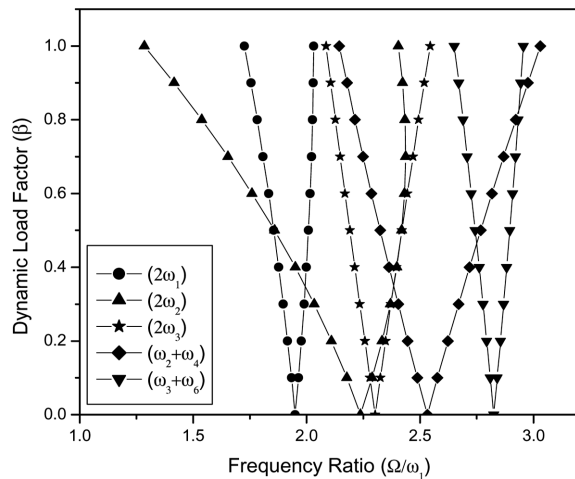Fig. 10 Same as Fig. 9, but for ($c/b = 0.8$)

Fig. 11 Regions of simple and combination resonances of spherical panel subjected to compressive partial edge loading at one end ($c/b = 0.2$, $\alpha = 0.2$)
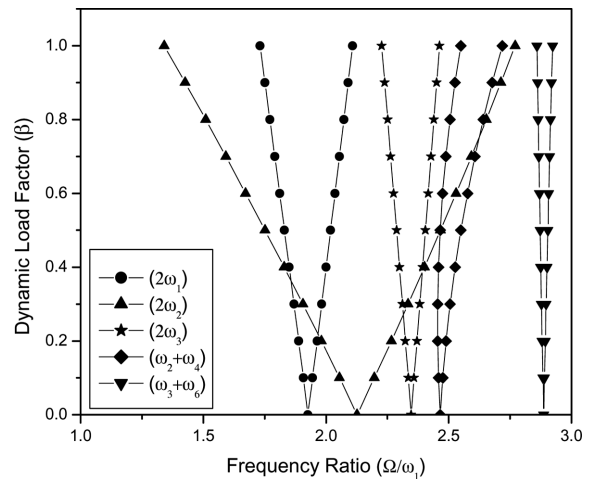

Fig. 12 Same as Fig. 11, but for ($c/b = 0.8$)

to the fact that for the small values of load bandwidth or for concentrated edge loading, the periodic term in Eq. (7) produces a strong modal coupling leading to the wider combination resonance zones. This signifies that the combination resonance zones have significant instability effects similar to the simple resonance behavior.

Having established the significance of the combination resonance instability along with simple resonance, the instability regions are plotted in Figs. 13-20, for different cases with regard to different parameters such as curvature, damping and the static load factor of the applied parametric edge loading of the doubly curved panels.
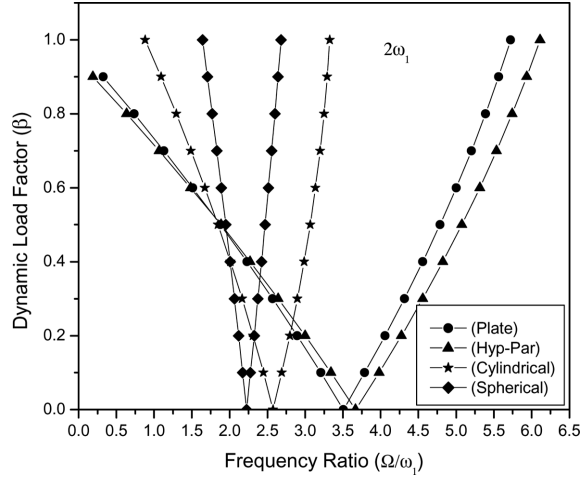
Fig. 13 Effect of curvature on simple resonance of the curved panels subjected to tensile partial edge loading at one end ($c/b = 0.8$, $\alpha = 0.2$)
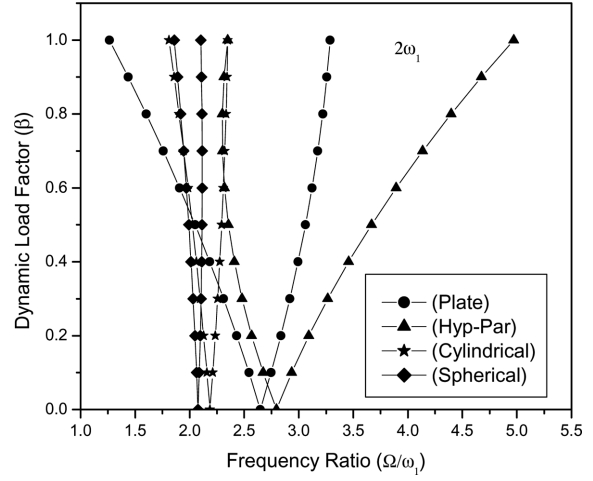
Fig. 14 Same as Fig. 13, but for tensile concentrated edge loading at one end ($c/b = 0.0$)

3.4 Effect of curvature

It has been observed from Figs. 13 and 14 that the excitation frequency decreases with introduction of curvatures from plate to doubly curved panel except hyperbolic paraboloid panel, the instability regions shift inward on the frequency ratio axis and their widths decrease. This indicates that the doubly curved panels are more susceptible to dynamic instability under tensile edge loading, but the dynamic instability behavior of hyperbolic paraboloid panel is similar to that of flat panel.
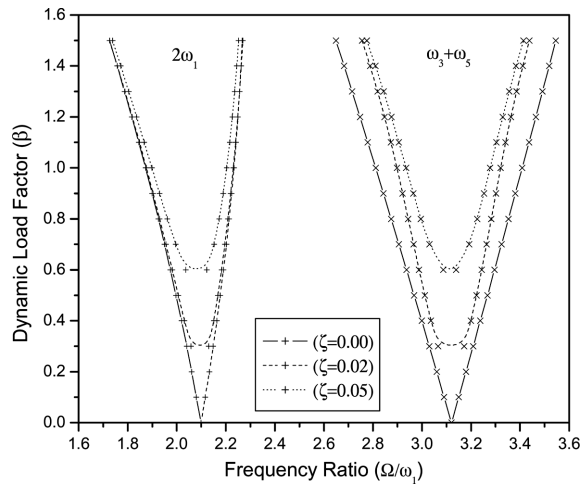

Fig. 15 Effect of damping on simple and combination resonances of spherical panel subjected to tensile partial edge loading at one end ($c/b = 0.2$, $\alpha = 0.2$)
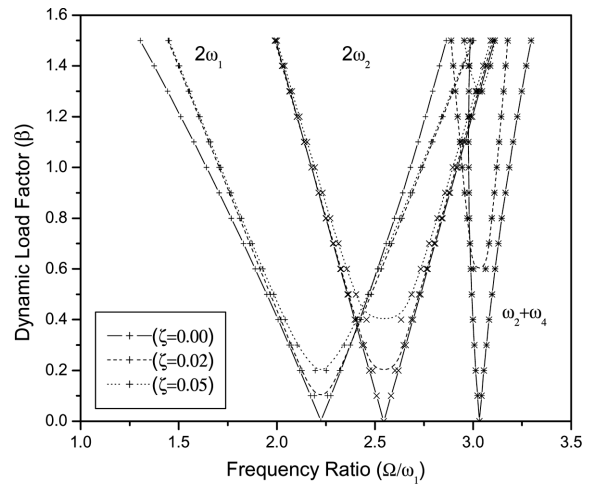
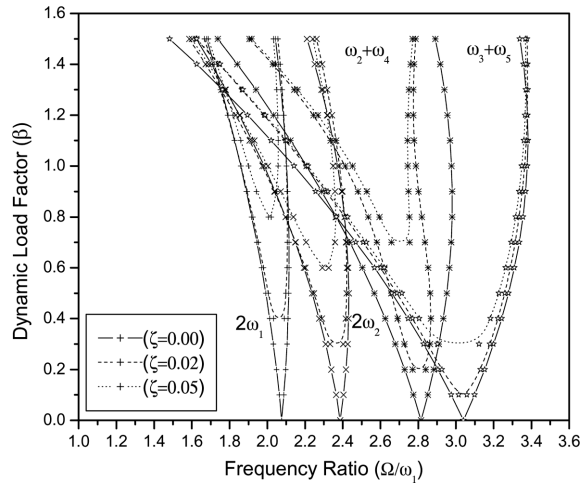Fig. 16 Same as Fig. 15, but for ($c/b = 0.8$)

Fig. 17 Effect of damping on simple and combination resonances of spherical panel subjected to tensile concentrated edge loading at one end ($c/b = 0.0$, $\alpha = 0.2$)
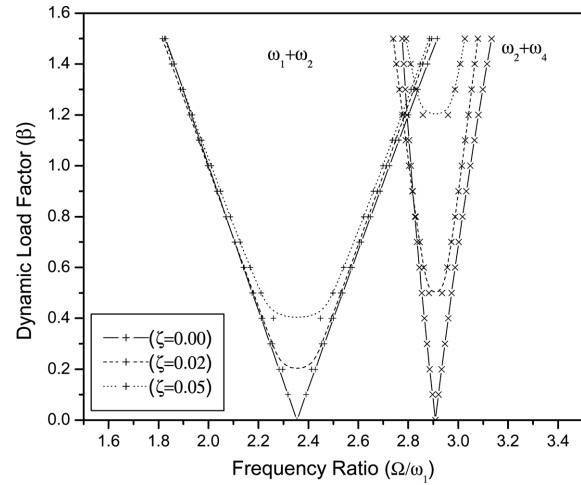
Fig. 18 Same as Fig. 17, but for concentrated edge loading near the centre ($c/b = 0.4$)

3.5 Effect of damping

It can be observed from Figs. 15-18 that the widths of instability regions in the presence of damping are smaller as compared to those without damping, but damping may have destabilizing effect on the instability regions for higher values of β. The damping has pronounced effects when the curved panel is subjected to localized tensile edge loading at one end ($c/b = 0.2$) or concentrated edge loading at one end ($c/b = 0.0$). It can be observed that due to presence of damping, there is a critical value of dynamic load factor β^* for each instability region below which the curved panel can not become dynamically unstable. The value of β^* increases as the modal damping ratio increases. The extent of the effect of damping on β^* also depends on the nature of the edge loading as can be observed from different load parameters. As the width of partial edge loading is increased or as the concentrated edge load is moved from one end to the centre, the critical dynamic load factor decreases, indicating more susceptibility to dynamic instability. Under uniform loading ($c/b = 0.8$) or for concentrated edge loading near the centre ($c/b = 0.4$), the critical dynamic load factor β^* may be so high for the combination resonance zones in the presence of damping with high modal damping ratio that the combination resonances can be neglected for practical purposes.

3.6 Effect of the static load factor

The effect of the static load factor on the instability regions can be observed from Figs. 19 and 20. The simple and combination resonance instability regions shift outward on the frequency ratio axis and their widths decrease. This indicates that the curved panels are less susceptible to dynamic instability due to higher static load, because the dynamic instability depends on the strength and area of compressive zones developed within the curved panels. It means that it has the stabilizing effect on the dynamic instability behavior of the doubly curved panels.
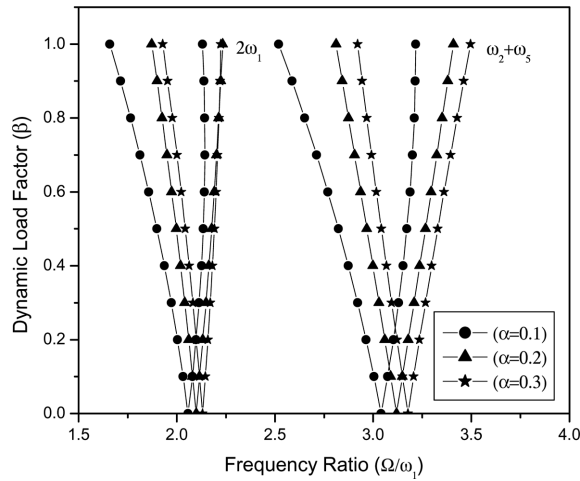
Fig. 19 Effect of static load factor on simple and combination resonances of spherical panel subjected to tensile partial edge loading at one end (*c/b* = 0.2)
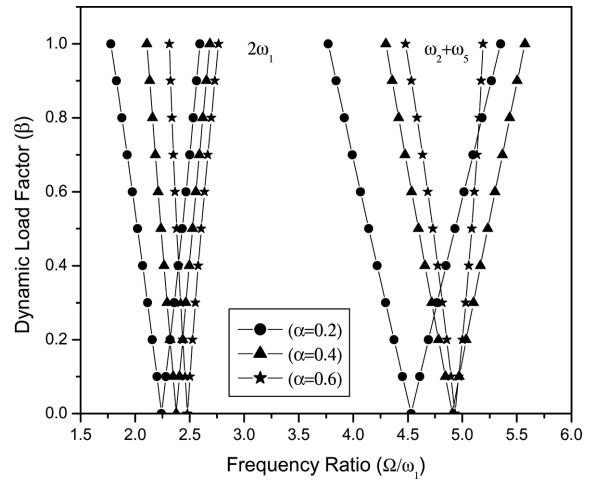

Fig. 20 Same as Fig. 19, but for cylindrical panel

4. Conclusions

The results from a study of the simple and combination resonance characteristics of the doubly curved panels subjected to tensile partial edge loading and concentrated edge loading can be summarized as follows.

- The doubly curved panels subjected to tensile non-uniform edge loading buckle due to compressive stresses developed within the curved panels. The value of the tensile buckling load depends on the strength and extent of the compressive zone.
- The combination resonance zone contributes a considerable amount to the total instability region and the widths of combination resonance zones are comparable to those of the simple resonance zones for the edge loading of small bandwidth or for concentrated edge loading.
- The widths of the combination resonance zones are large for the partial edge loading of small bandwidth or for concentrated edge loading and are very small for nearly uniform loading, but the widths of simple resonance zones are smaller for localized edge loading of small bandwidth or for concentrated edge loading at one end. The reason is attributed to the edge restraining effect.
- The dynamic instability results under tensile periodic edge loading show that the instability regions occur at higher frequency ratios in contrast to the corresponding compressive loading cases. The effect of position of loading on the edge is similar to that of compressive loading case.
- The instability regions shift inward on the frequency ratio axis and their widths decrease with introduction of curvatures from plate to doubly curved panel. This indicates that the doubly curved panels except hyperbolic paraboloid panel are more susceptible to dynamic instability under tensile edge loading.
- The effect of damping on the instability regions is stabilizing and it may be destabilizing for

higher values of dynamic load factor. There is a critical value of dynamic load factor for each instability region below which the curved panel is not susceptible to dynamic instability. As the modal damping ratio increases, the critical dynamic load factor increases.

- For nearly uniform loading or for concentrated loading near the centre, the critical dynamic load factor with high modal damping ratio for combination resonance zone become so high that combination resonance effects may not be of practical interest.

- The curved panels are less susceptible to dynamic instability due to higher static load, because the compressive stresses developed within the curved panels are not very effective to cause the dynamic instability.

References

Argento, A. (1993), "Dynamic stability of a composite circular cylindrical shell subjected to combined axial and torsional loading", *J. Compos. Mater.*, **29**(11), 2000-2005.

Argento, A. and Scott, R.A. (1993), "Dynamic instability of layered anisotropic circular cylindrical shells, part I: Theoretical development", *J. Sound. Vib.*, **162**(2), 311-322.

Bolotin, V.V. (1964), *The Dynamic Stability of Elastic Systems*, Holden-Day, San Francisco.

Bolotin, V.V., Grishko, A.A. and Panov, M.Y. (2002), "Effect of damping on the postcritical behaviour of autonomous non-conservative systems", *Non-Linear. Mech.*, **37**, 1163-1179.

Cederbaum, G. (1991), "Dynamic instability of shear-deformable laminated plates", *AIAA J.*, **29**(11), 2000-2005.

Choo, Y.S. and Kim, J.H. (2000), "Dynamic stability of rectangular plates subjected to pulsating follower forces", *AIAA J.*, **38**(2), 353-361.

Deolasi, P.J. and Datta, P.K. (1995), "Effects of damping on the parametric instability behaviour of plates under localized edge loading (compression or tension)", *Struct. Eng. Mech.*, **3**(3), 229-244.

Deolasi, P.J. and Datta, P.K. (1997), "Simple and combination resonances of rectangular plates subjected to non-uniform edge loading with damping", *Eng. Struct.*, **19**(12), 1011-1017.

Engel, R.S. (1991), "Dynamic stability of an axially loaded beam on elastic foundation with damping", *J. Sound Vib.*, **146**(3), 463-477.

Hsu, C.S. (1963), "On the parametric excitation of dynamic system having multiple degrees of freedom", *J. Appl. Mech.*, ASME, **30**(3), 367-372.

Hutt, J.M. and Salam, A.E. (1971), "Dynamic stability of plates by finite element method", *J. Eng. Mech. Div.*, ASCE, **97**, 879-899.

Iwatsubo, T., Sugiyama, Y. and Ogino, S. (1974), "Simple and combination resonances of columns under periodic axial loads", *J. Sound Vib.*, **33**(2), 211-221.

Kar, R.C. and Sujata, T. (1991), "Dynamic stability of a tapered symmetric sandwich beam", *Comput. Struct.*, **40**(6), 1441-1449.

Kim, J.H. and Choo, Y.S. (1998), "Dynamic stability of a free-free Timoshenko beam subjected to a pulsating follower force", *J. Sound Vib.*, **216**(4), 623-636.

Lee, W.K. and Kim, C.H. (1995), "Combination resonances of a circular plate with three-mode interaction", *J. Appl. Mech.*, ASME, **62**, 1015-1022.

Leissa, A.W. and Ayoub, E.F. (1989), "Tension buckling of rectangular sheets due to concentrated forces", *J. Eng. Mech.*, ASCE, **115**(12), 2749-2762.

Leissa, A.W., Lee, J.K. and Wang, A.J. (1983), "Vibrations of cantilevered doubly curved shallow shells", *Int. J. Solids. Struct.*, **19**(5), 411-424.

Matsunaga, H. (1999), "Vibration and stability of thick simply supported shallow shells subjected to in-plane stresses", *J. Sound Vib.*, **225**(1), 41-60.

Mond, M. and Cederbaum, G. (1992), "Dynamic instability of anti-symmetric laminated plates", *J. Sound Vib.*, **154**(2), 271-279.

Cederbaum, G. (1992), "Analysis of parametrically excited laminated shells", *Int. J. Mech. Sci.*, **34**(3), 241-250.

Moorthy, J., Reddy, J.N. and Plaut, R.H. (1990), "Parametric instability of laminated composite plates with transverse shear deformation", *Int. J. Solids Struct.*, **26**, 801-811.

Nayfeh, A.H. (1973), *Perturbation Methods,* Wiley, New York.

Nayfeh, A.H. and Mook, D.T. (1979), *Nonlinear Oscillations,* Wiley, New York.

Ostiguy, G.L., Samson, L.P. and Nguyen, H. (1993), "On the occurrence of simultaneous resonances in parametrically-excited rectangular plates", *J. Vib. Acoust.*, **115**(3), 344-352.

Saha, K.N., Kar, R.C. and Datta, P.K. (1997), "Dynamic stability of a rectangular plate on non-homogeneous Winkler foundation", *Comput. Struct.*, **63**(6), 1213-1222.

Sahu, S.K. and Datta, P.K. (2001), "Parametric instability of doubly curved panels subjected to non-uniform harmonic loading", *J. Sound Vib.*, **240**(1), 117-129.

Szemplinska-Stupnicka, W. (1978), "The generalized harmonic balance method for determining the combination resonance in the parametric dynamic systems", *J. Sound Vib.*, **58**(3), 347-361.

Takahashi, K. (1981), "An approach to investigate the instability of the multiple degree of freedom parametric dynamic systems*", J. Sound Vib.*, **78**(4), 519-529.

Takahashi, K. and Konishi, Y. (1988), "Dynamic stability of a rectangular plate subjected to distributed in-plane dynamic force", *J. Sound Vib.*, **123**(1), 115-127.

Notation

a, b : Panel lengths in X and Y-direction respectively

c : Load parameter

$[C]$: Damping matrix

D : Flexural rigidity of the panel

E : Modulus of elasticity

G : Shear modulus

h : Thickness of the panel

$[K]$: Elastic stiffness matrix

$[M]$: Mass matrix

P : Edge Load

P_{cr} : Static buckling Load

$\{q\}$: Nodal displacement

R_x, R_y : Radii of curvatures in X and Y-direction respectively

$[S]$: Stress stiffness matrix

t : Time

x, y, z : Cartesian co-ordinates

α, β : Static and dynamic load factors respectively

σ : Detuning parameter

ρ : Mass density of the material
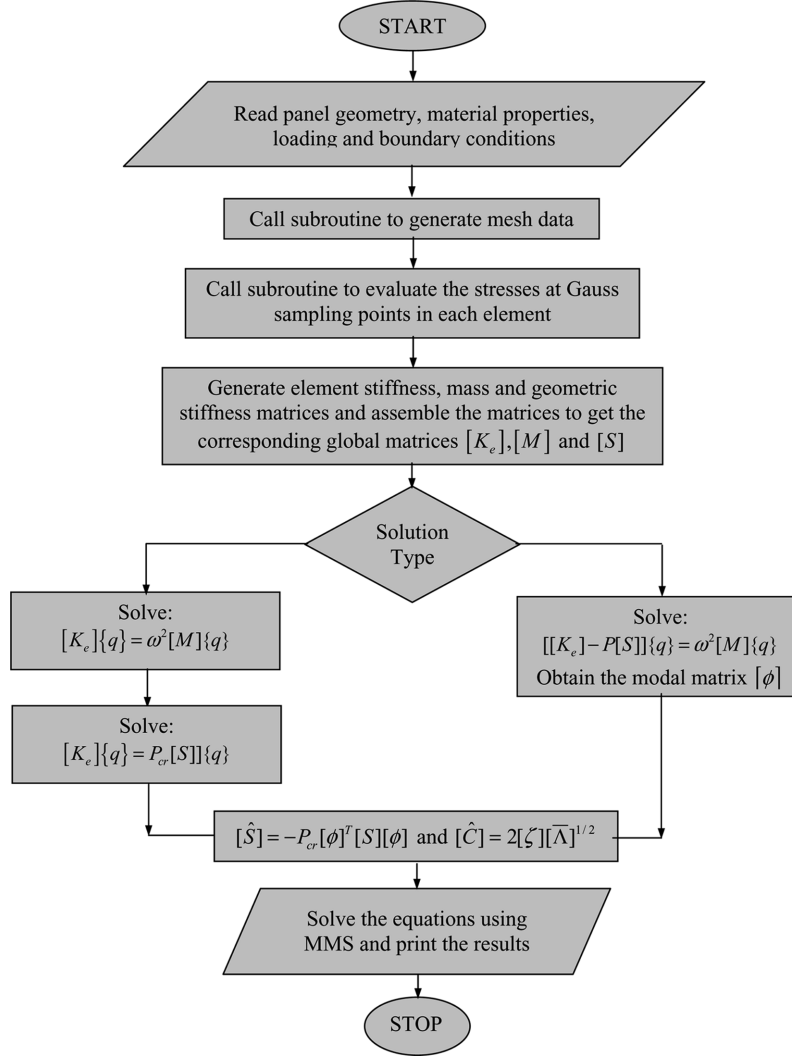
ν : Poisson's ratio

Ratnakar. S. Udar and P. K. Datta

Appendix-I

Fig. 1 Flow chart of the computer program